

Supplementary information to *light absorption and albedo reduction by pigmented microalgae on snow and ice*

Lou-Anne CHEVROLLIER,¹ Joseph M. COOK,¹ Laura HALBACH,¹ Hans JAKOBSEN,² Liane G. BENNING,^{3,4} Alexandre M. ANESIO,¹ Martyn TRANTER¹

¹*Aarhus University, Department of Environmental Science, iClimate, Roskilde, Denmark*

²*Aarhus University, Institut for Ecoscience, Roskilde, Denmark*

³*German Research Centre for Geosciences, GFZ, Potsdam, Germany*

⁴*Free University of Berlin, Department of Earth Sciences, Berlin, Germany*

Correspondence: Lou-Anne Chevrollier <lou.chevrollier@envs.au.dk>

METHODS

Sampling collection and processing

Snow samples were collected between July 19th and August 9th 2021 and left on the ice surface until complete melt when they were transferred to incubation bottles (Falcon™, Fisher Scientific), and ice samples were collected on August 9th 2021. Particulates were concentrated from melted snow and ice samples by repeated centrifugation at 10400 rpm. Algal cells were isolated from these concentrates by repeated density gradient centrifugation at 500g for 5-10mn with a double layer system of Iodixanol (Optiprep, StemCell; 60/24% Iodixanol for ice algae and 40/5% Iodixanol for snow algae). Algal isolates were then rinsed by centrifugation at 10400 rpm 3-4 times until the UV-absorption signature of Iodixanol disappeared in the spectrophotometric measurements. Once cleaned, the isolates were resuspended again in cold water.

In vivo absorption cross sections: measurements and calculations

The measurements were carried at different acquisition speeds and no difference was observed in the signal, except for the noise that was more important for high speed acquisition. In addition, no significant accumulation of cells was observed at the bottom of the cuvette after the measurement, indicating that the bias introduced from cell sinkage was likely minimal. The volumes of the suspensions used for measurements were large (50 - 120mL) to ensure a wide variety of cells and kept in an ice bath during the analysis to

26 avoid pigment leakage and stress. Prior to measurement, the cuvette was rinsed with the sample, closed
27 with a clean PTFE lid, the windows were cleaned with fiber-free paper, and the solution in the cuvette
28 was stirred to reduce the bias induced by particle settling. All transmission measurements were carried in
29 triplicates directly after. The transmission spectra of the filtrates were also measured and used to correct
30 the transmission spectra of the algal suspension from pigment leakage. 1mL of the solution was used
31 to perform algal cell counts (cells mL⁻¹), systematically counting two entire lines from the upper and
32 lower part of the chamber (1 mL, Marienfeld Superior™ Sedgewick Rafter) placed under Nikon Eclipse Ti
33 microscope, that was also used to image the cells. The absorbance calculation follows the equation from
34 (Kandilian and others, 2016), except that we did not apply a spectral correction for the scattering but a
35 constant or “baseline” correction as in (Bidigare and others, 1990). The baseline correction is normally
36 typically applied at 750nm (Bidigare and others, 1990), but snow algae absorb also in the near-IR (Gorton
37 and others, 2001) and the ice algal signature in field spectra was also visible in the near IR, making
38 the correction at 800nm more appropriate. For both algae, A_λ was calculated from three independent
39 suspensions collected at different sites in different days of the study area, while $A_{\lambda,m}$ was calculated from
40 two of them only because mass quantification was not performed for the last suspension. Cell sizes (μm) and
41 biovolumes ($\mu\text{m}^3 \text{ cell}^{-1}$) were measured using a FlowCam (Fluid Imaging Technologies Inc., fluid imaged 0.1
42 to 0.2 mL). Snow algae diameters (μm) were directly obtained from the instrument for each sample (n_{total}
43 = $3.1 \cdot 10^4$ cells), which calculates a pixel area reconstructed diameter (ABD), and biovolumes ($\mu\text{m}^3 \text{ cell}^{-1}$)
44 were calculated from the diameter assuming a spherical shape. Ice algae lengths and widths were measured
45 from the FlowCam images using ImageJ (Version 1.53; $n_{total} = 973$ cells) and biovolumes were calculated
46 assuming a circular-based cylinder shape following (Williamson and others, 2018) after (Hillebrand and
47 others, 1999). The algal buoyant density was determined by immersing algae in solutions of Iodixanol
48 (Optiprep, Stem Cell, Proteogenix) of increasing densities (Alere Technologies: <https://goo.gl/I4owRU>)
49 until the cells floated.

50 **In vitro absorption cross section: measurements and calculations**

51 The lipophilic phase was first extracted from the filters with a solution of methyl tertiary-butyl ether
52 (MTBE) with 0.1% of butylated hydroxytoluene (BHT). Then, the lipophilic and hydrophilic phases were
53 extracted using a double layer system with the previous solution and a solution of MeOH 20%. Third,
54 extraction of the hydrophilic phase with MeOH 20% alone was performed as in (Halbach and others, 2022).

55 We then added five additional double phase extraction steps with both solvents until the extracts were not
56 visibly colored anymore, to ensure complete extraction. All steps were performed under a fume hood in
57 the dark. These reconstructed coefficients were calculated from 300nm and not 240nm because MTBE is
58 highly absorbing at lower wavelengths which biases the transmission measurements.

59 **Calculation and modelling of algal single scattering properties**

60 The real part of the refractive index n_λ was estimated by optical densitometry following (Hart and Leski,
61 2006). Briefly, isolated algae were resuspended in 25, 30, 35, 40 and 45% of Iodixanol and transmission
62 spectra of these solutions were measured. The algal refractive index was determined from the refractive
63 index of the solution showing maximal transmission at 800nm. The refractive indices of the different
64 solutions were calculated from (Boothe and others, 2017).

65 **Albedo modelling and melt calculations**

66 The range of density values used for the LUT was 300 to 900 kg m⁻³ with a step of 20 kg m⁻³ and
67 corresponded to the range measured at the field site in the same period (unpublished data). The range
68 of effective radii for the bubble inclusions was 1000 to 20,000 μm with a step of 500 μm . The underlying
69 boundary reflectance of the model was constrained with a spectrum from a blue polished ice surface
70 measured at our field site, so that the depth represented the distance to the water table and varied from 3
71 to 20.5 cm. The solar zenith angle (SZA) was calculated from the time of acquisition of the measurements
72 ([http://solardat.uoregon.edu/cgi-bin/
73 SolarPositionCalculator.cgi](http://solardat.uoregon.edu/cgi-bin/SolarPositionCalculator.cgi)). A manual second-step adjustment for the ice parameters was performed using
74 in-between parameters to reduce the error further. The sampling depth correction varied between 0 and
75 6cm due to the inaccuracy in sampling surface ice and the different sampling methods used (ice screw, ice
76 axe). Since it was not measured in our study, it was manually tuned to minimize the error in broadband
77 albedo (BBA, unitless) in the visible spectrum.

78 Figures were produced using matplotlib and the color maps from (van der Velden, 2020).

79 **FIGURES AND TABLES**

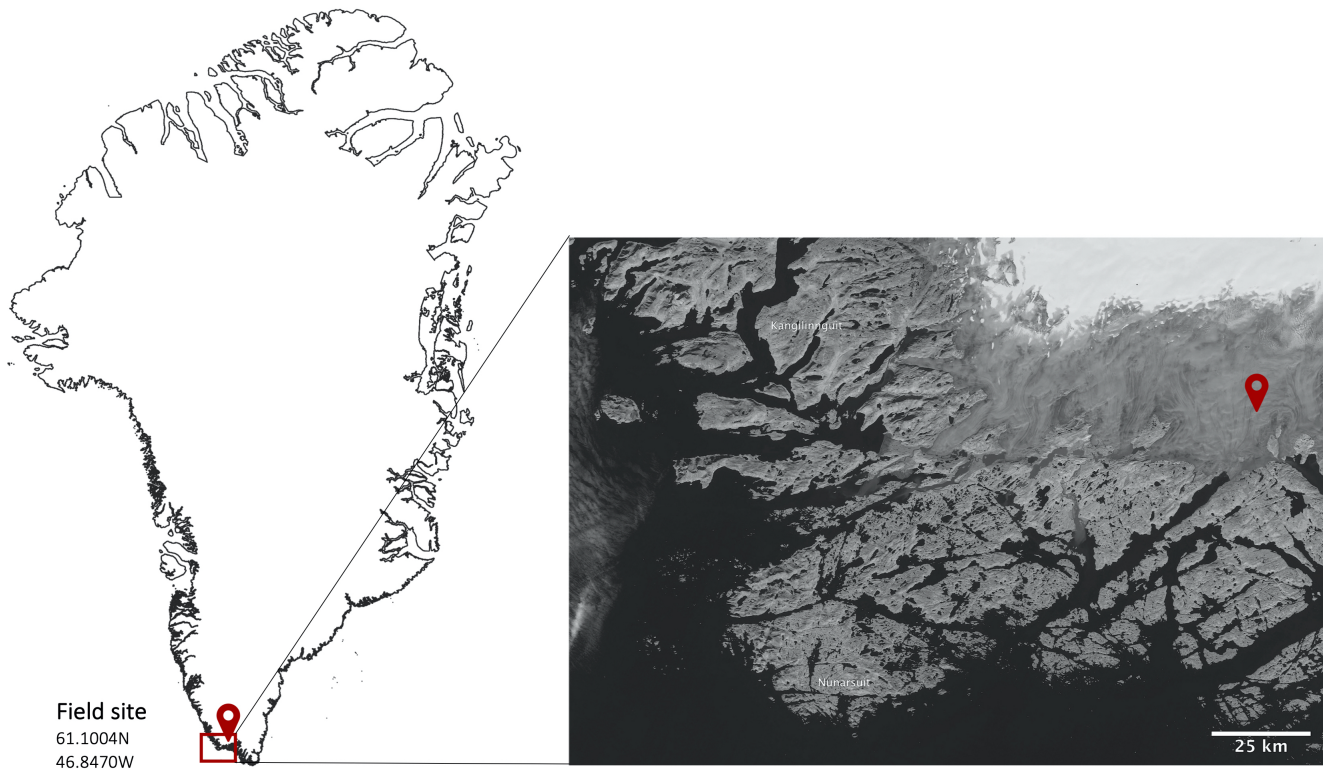


Fig. S1. Map indicating the study area in south Greenland. The satellite image is from the tile T23VLH from 22.08.21.

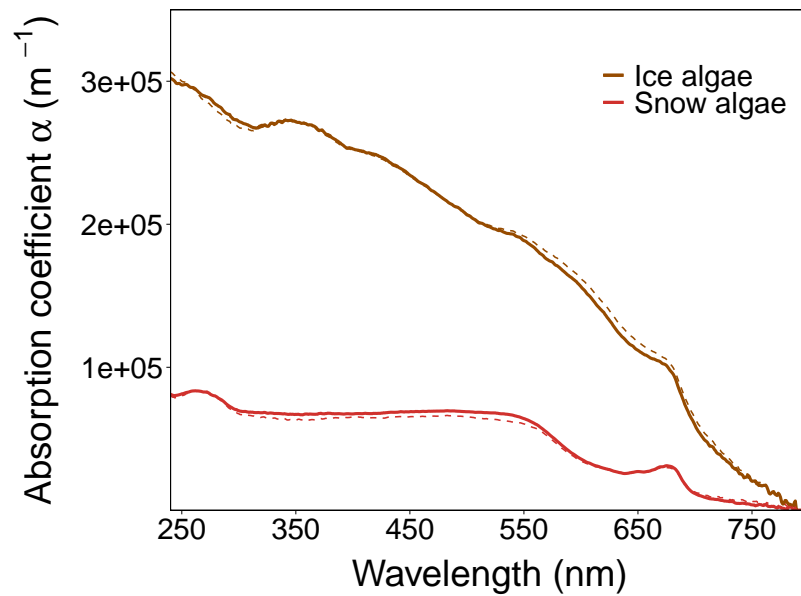


Fig. S2. Mean absorption coefficient a_{λ} of snow and ice algae calculated from $A_{\lambda,m}$ (solid line) and A_{λ} (dashed line).

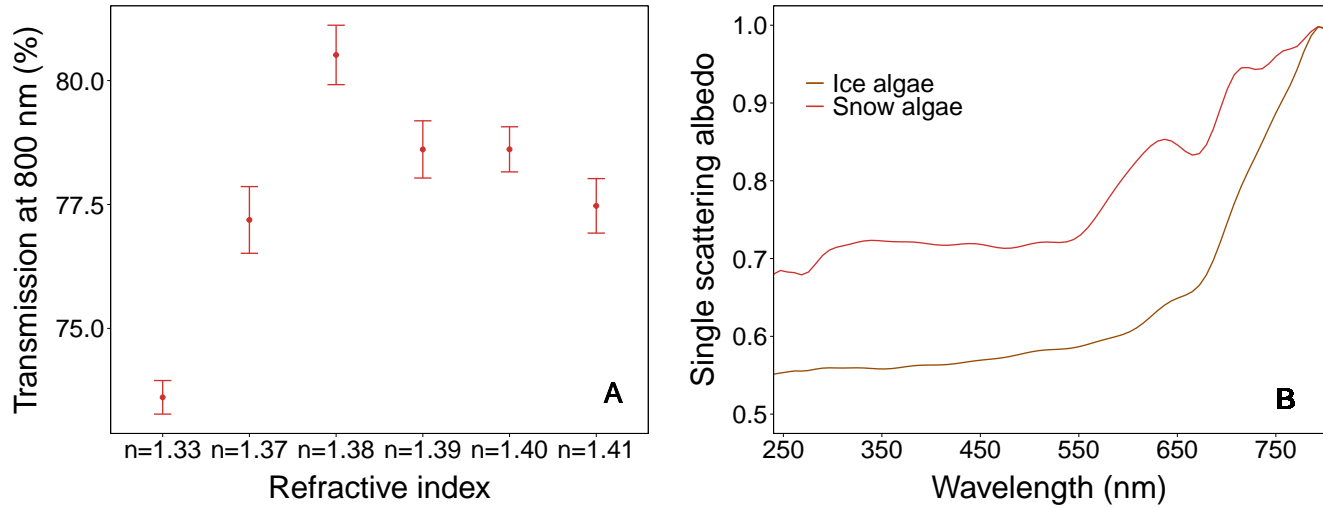


Fig. S3. (a) Optical densitometry results for snow algae cells, indicating a maximum transmission for a refractive index of 1.38, really close to theoretical estimations (Dauchet and others, 2015). For ice algae, this could not be measured and we used the same value of 1.38. (b) the single scattering albedos of both algal cells (smoothed line).

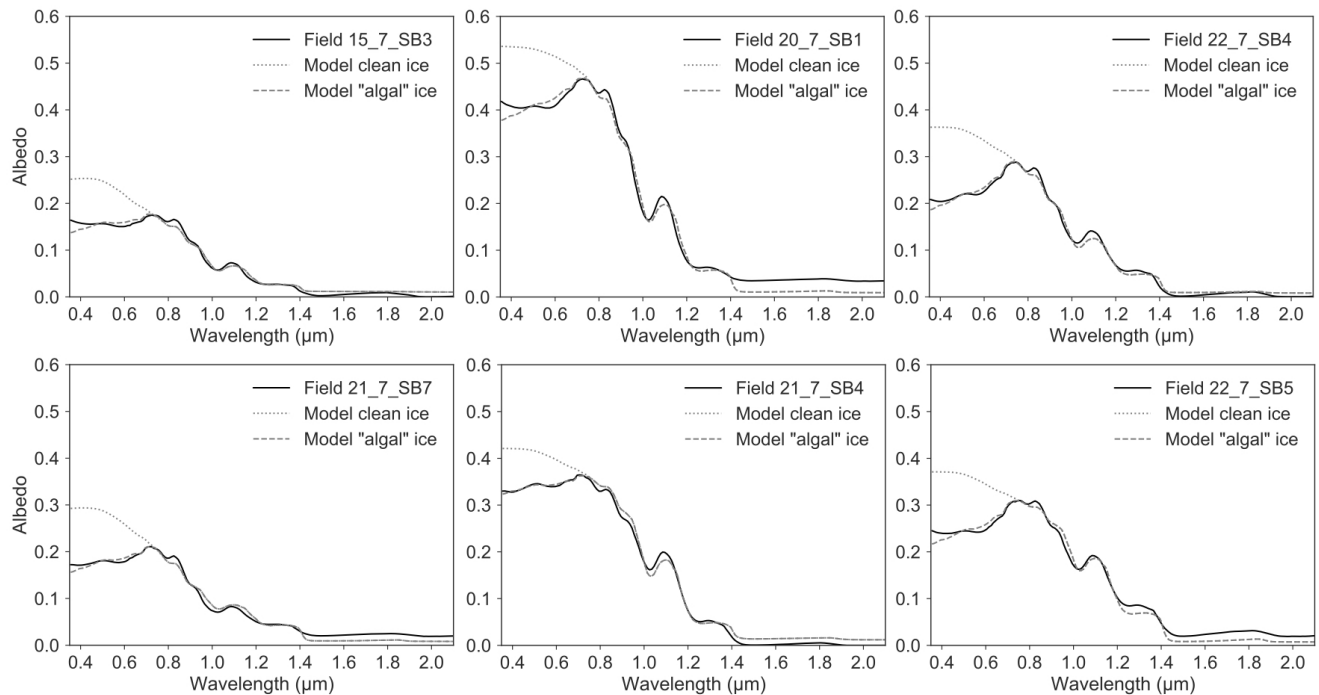


Fig. S4. Additional comparisons of model outputs vs field spectra for sites from the Dark Zone of Greenland from (Cook and others, 2020).

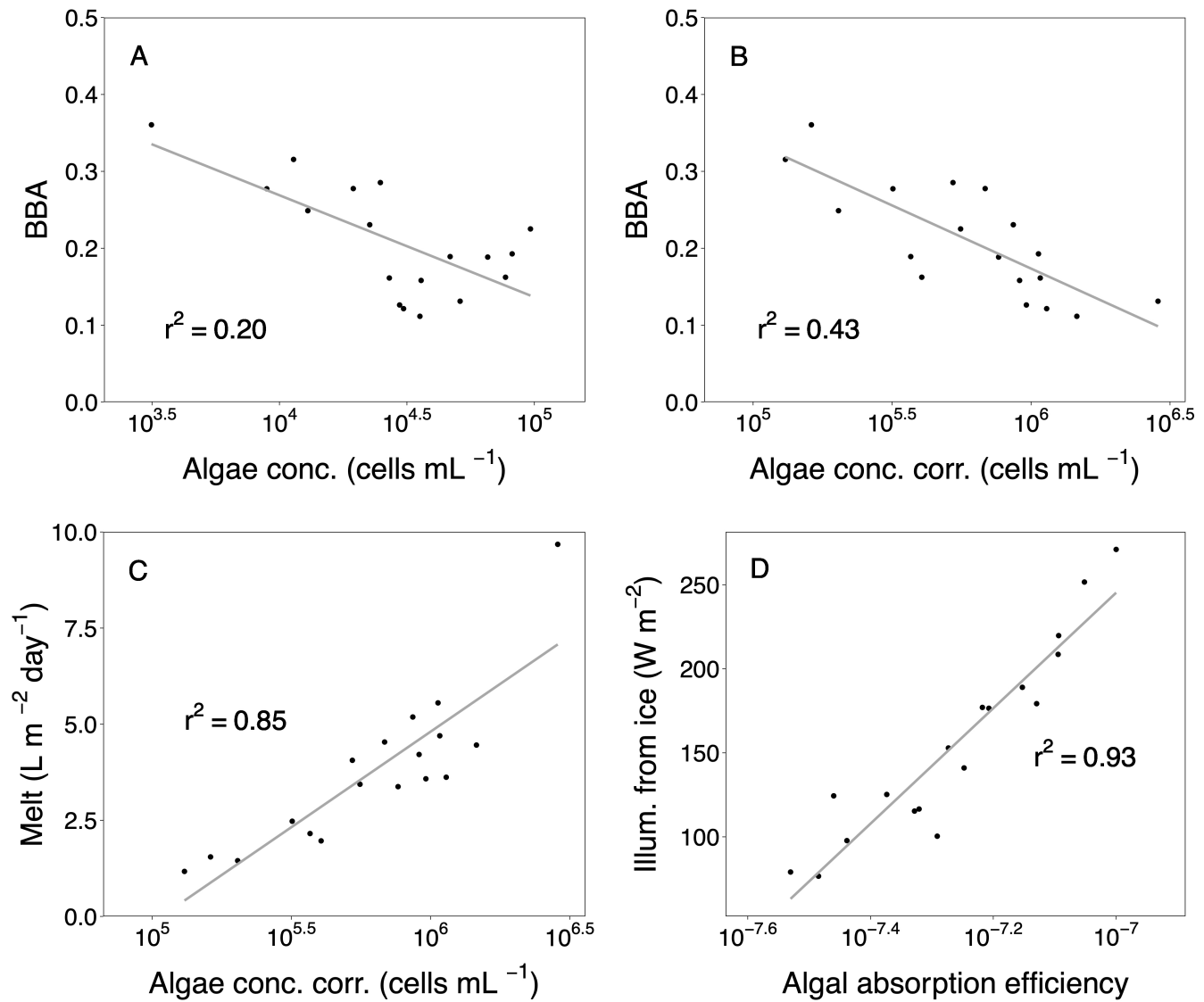


Fig. S5. (a) Correlation between the measured BBA and algal concentration measured in the field, (b) correlation between the measured BBA and algal concentration corrected for the sampling depth (see Table S4), (c) correlation between the daily melt generated and algal concentration corrected for the sampling depth (see Table S4), (d) correlation between the illumination received from the ice and the algal absorption efficiency, defined as the ratio between BBA reduction and algal concentration corrected for the sampling depth.

Table S1. Mean and SD values for cell sizes of snow algae analysed for optical properties, along with the dry weight. Letters indicate replicates and number indicate independent samples. Dry weights indicated as (calc) correspond to values calculated by multiplying biovolumes with dry density.

Sample ID	Diameter (μm)	Biovolume (μm^3)	Nb of cells imaged	Dry weight (ng cell^{-1})
snow1a	15.96 ± 2.28	2129	2802	(calc: 1.33)
snow1b	15.96 ± 2.16	2129	2318	0.98 (calc: 1.33)
snow1c	16.20 ± 2.34	2226	2444	(calc: 1.39)
snow2a	16.80 ± 2.82	2483	616	(calc: 1.55)
snow2b	16.90 ± 2.91	2527	649	(calc: 1.58)
snow2c	17.14 ± 3.76	2637	621	(calc: 1.65)
snow3a	19.33 ± 3.89	3782	4410	(calc: 2.36)
snow3b	20.61 ± 5.21	4584	4338	(calc: 2.87)
snow3c	22.04 ± 7.19	5606	10657	2.26 (calc: 3.50)
snow3d	19.80 ± 4.80	4064	2346	(calc: 2.54)

Table S2. Mean and SD values for cell sizes of ice algae analysed for optical properties, along with the dry weight (only available for the suspension which yielded the average absorption cross section). Dry weights indicated as (calc) correspond to values calculated by multiplying biovolumes with dry density.

Sample ID	Width (μm)	Length (μm)	Biovolume (μm^3)	Nb of cells imaged	Dry weight (ng cell^{-1})
ice2a	9.52 ± 1.15	19.23 ± 4.95	1398 ± 531	418	(calc: 0.96)
ice2b	9.61 ± 1.08	19.21 ± 5.89	1416 ± 563	288	0.93 (calc: 0.97)
ice2c	10.36 ± 0.97	17.74 ± 4.22	1521 ± 525	268	(calc: 1.04)

Table S3. Values for the model parameters used for the simulations of ice and snow algal blooms.

Surface type	Density (kg m^{-3})	r_{eff} (μm)	Depth (m)	Solar zenith angle	Sampling depth (cm)	Algal conc. (cells mL^{-1})
Ice	650, 700	3000, 3500	0.05, 0.06	45	2	5000,10000,
	750, 800	4000, 4500	0.07, 0.08			15000, ...,
	850	5000, 5500	0.09, 0.1			150000
Snow	400, 450	1500, 2000	0.05, 0.06	45	2	5000,10000,
	500, 550	2500, 3000	0.07, 0.08			15000, ...,
	600	3500, 4000	0.09, 0.1			150000

Table S4. Values for the model parameters used for the inversions of field spectra. SA = snow algae, IA = ice algae, SE = mean standard error. *concentrations not measured.

Sample ID	Density (kg m ⁻³)	r_{eff} (μm)	Depth (m)	Solar zenith angle	Sampling depth (cm)	IA conc. (cells mL ⁻¹)	SA conc. (cells mL ⁻¹)	BBA red.	SE albedo
050821-S2	700	2500	0.08	44	1.15	11360	0	0.012	0.006
050821-S3	700	2500	0.074	47	2.11	24880	0	0.042	0.008
050821-S4	840	3500	0.14	47	0.79	46720	0	0.021	0.008
050821-S7	580	4500	0.047	48	1.3	81800	0	0.057	0.004
050821-S8	780	5000	0.074	49	0.525	77040	0	0.019	0.002
060821-S1	680	8000	0.055	49	3.25	29440	160	0.035	0.009
060821-S2	700	2500	0.051	47	3.82	22600	0	0.054	0.012
060821-S3	600	4500	0.060	47	1.57	12800	120	0.014	0.004
060821-S4	840	15500	0.35	46	3.06	20000*	0*	0.023	0.009
060821-S5	740	3000	0.041	46	4.0	26780	200	0.046	0.006
060821-S6	900	2000	0.14	45	3.71	29320	1360	0.034	0.011
060821-S7	720	2500	0.05	45	0.578	96080	440	0.034	0.004
060821-S9	580	4000	0.038	45	5.60	51000	120	0.099	0.008
060821-S10	880	6500	0.24	46	2.45	42000*	0*	0.031	0.003
060821-S11	580	2500	0.062	47	5.15	3147	0	0.016	0.004
060821-S12	460	6000	0.071	49	3.57	8840	80	0.026	0.010
060821-S13	800	5000	0.11	50	2.53	35893	53	0.043	0.007
060821-S14	680	2000	0.043	52	3.51	19360	120	0.051	0.012
060821-S15	800	6000	0.071	53	4.11	35360	200	0.048	0.009
060821-S16	800	2500	0.044	56	1.165	65320	280	0.039	0.006
15-7-SB3	820	4000	0.073	47	4.08	30313	0	0.043	0.006
20-7-SB1	580	2500	0.07	48	5.68	11375	0	0.061	0.018
22-7-SB4	360	6000	0.061	47	3.36	14313	0	0.037	0.009
21-7-SB7	880	2000	0.115	48	3.99	33229	0	0.052	0.009
21-7-SB4	800	2000	0.062	48	2.375	57083	0	0.070	0.006
22-7-SB5	720	1500	0.028	47	4.85	22813	0	0.060	0.012

80 **REFERENCES**

- 81 Bidigare RR, Ondrusek ME, Morrow JH and others (1990) In-vivo absorption properties of algal pigments. *Ocean*
82 *Optics X*, **1302**, 290–302 (doi: <https://doi.org/10.1117/12.21451>)
- 83 Boothe T, Hilbert L, Heide M and others (2017) A tunable refractive index matching medium for live imaging cells,
84 tissues and model organisms. *Elife*, **6**, e27240 (doi: <https://doi.org/10.7554/eLife.27240>)
- 85 Cook JM, Tedstone AJ, Williamson CJ and others (2020) Glacier algae accelerate melt rates on the south western
86 greenland ice sheet. *The Cryosphere*, **14(1)**, 309–330 (doi: <https://doi.org/10.5194/tc-14-309-2020>)
- 87 Dauchet J, Blanco S, Cornet JF and others (2015) Calculation of the radiative properties of photosyn-
88 thetic microorganisms. *Journal of Quantitative Spectroscopy and Radiative Transfer*, **161**, 60–84 (doi:
89 <https://doi.org/10.1016/j.jqsrt.2015.03.025>)
- 90 Gorton HL, Williams WE and Vogelmann TC (2001) The light environment and cellular optics of the
91 snow alga *Chlamydomonas nivalis* (Bauer) Wille. *Photochemistry and Photobiology*, **73(6)**, 611–620 (doi:
92 [https://doi.org/10.1562/0031-8655\(2001\)0730611TLEACO2.0.CO2](https://doi.org/10.1562/0031-8655(2001)0730611TLEACO2.0.CO2))
- 93 Halbach L, Chevrollier LA, Doting E and others (2022) Pigment signatures of algal communities and their implications
94 for glacier surface darkening, in review. *Scientific reports*, **X**, X
- 95 Hart SJ and Leski TA (2006) Refractive index determination of biological particles. Technical report, Naval Research
96 Lab Washington DC
- 97 Hillebrand H, Dürselen CD, Kirschtel D and others (1999) Biovolume calculation for pelagic and benthic microalgae.
98 *Journal of phycology*, **35(2)**, 403–424 (doi: <https://doi.org/10.1046/j.1529-8817.1999.3520403.x>)
- 99 Kandilian R, Soulies A, Pruvost J and others (2016) Simple method for measuring the spec-
100 tral absorption cross-section of microalgae. *Chemical Engineering Science*, **146**, 357–368 (doi:
101 <https://doi.org/10.1016/j.ces.2016.02.039>)
- 102 van der Velden E (2020) CMasher: Scientific colormaps for making accessible, informative and 'cmashing' plots. *The*
103 *Journal of Open Source Software*, **5(46)**, 2004 (doi: [10.21105/joss.02004](https://doi.org/10.21105/joss.02004))
- 104 Williamson CJ, Anesio AM, Cook JM and others (2018) Ice algal bloom development on the surface of the greenland
105 ice sheet. *FEMS microbiology ecology*, **94(3)**, fyy025 (doi: <https://doi.org/10.1093/femsec/fyy025>)